

COVER SHEET

Title: *The performance of structural steel beams subject to a localized fire*

Authors* : Lisa Choe, Selvarajah Ramesh, Chao Zhang, John Gross

* National Institute of Standards and Technology, 100 Bureau Dr, Gaithersburg, Maryland 20899, USA
lisa.choe@nist.gov, selvarajah.ramesh@nist.gov, chao.zhang@nist.gov, john.gross@nist.gov

ABSTRACT

This paper presents the results from the open flame, localized fire tests conducted on 6.17 m long, simply supported W16×26 beam specimens. The cross sections at midspan (i.e., expected plastic hinge zone) of the beam specimen were directly exposed to the natural gas fire. Two different tests were conducted: (1) fire-thermal tests to evaluate the effects of the prescribed heat release rates (HRR), provided by the 1 m² natural gas burner, on the thermal responses of the specimen and (2) structural-fire test to evaluate the fire effects on the overall behavior and the load-bearing capacity of the specimen. The test results indicated that the prescribed heat release rates from the burner affected the heating rate of the specimen. When the HRR-time relationship of the burner followed a step function, the fire-exposed region of the beam specimen was heated essentially linearly with increasing time of fire exposure. When the HRR was set to a target magnitude of 400 kW throughout the test, the fire-exposed region was heated nonlinearly until it reached a steady-state temperature condition. When the beam specimen was subjected to linearly increasing flexural loads at a maintained HRR of 700 kW, combined flexural and lateral torsional failure of the specimen was exhibited. The lateral deformations in the compression flange at the fire-exposed critical sections initiated at (124 ± 5) kN-m, which is 39% of the plastic moment capacity at room temperature. The peak moment capacity was (171 ± 9) kN-m (54 % of the plastic moment capacity at room temperature), while the maximum temperature was (642 ± 28) °C at the HRR of 700 kW. The test results from the present study can be used for developing or calibrating analytical models, which can be eventually used for evaluating the performance of structural members subjected to a localized fire.

INTRODUCTION

The 6.17 m long W16×26 beam specimens subjected to a localized fire were tested at the National Fire Research Laboratory (NFRL) [1] of the National Institute of Standards and Technology (NIST). The main objective of these tests was to commission the structural fire experimental measurement capabilities of the newly constructed laboratory. A secondary objective was to generate data set for validation of analytical models. The experimental tests were divided into two parts: the fire-

thermal tests and the structural-fire test. The fire-thermal tests were intended to evaluate temperature-time responses of the steel beam specimen exposed to an open flame, localized fire with controlled heat release rates (HRR). No structural load was applied except the self-weight of the beam specimen. The structural-fire test was conducted such that the flexural loads and the open flame fire were applied to the critical sections (i.e., expected plastic hinge zone) of the specimen to evaluate the behavior and the flexural strength of the simply supported steel beam specimen.

FIRE-THERMAL TEST

Test setup, test protocol, and instrumentation layout

Figure 1 shows the test setup under the exhaust hood (13.7 m × 15.2 m) in the NFRL structural fire test bay. The W16×26 beam specimen of ASTM A992 steel [2] was placed on seated connections which were bolted to the W12×106 reaction column assemblies. Nominal dimensions of the W16×26 and W12×106 shapes are provided in ANSI/AISC 360-10 [3]. The fuel delivery system consisted of two natural gas burners with a nominal flame zone of one square meter to provide heat release rate (HRR) up to 1.5 MW. The uncertainty in the HRR measurements with a natural gas burner is presented in Bryant et al. [4] and not presented here for brevity. The distance from the lower flange of the beam specimen to the strong floor was 1.6 m. The assembled burner was placed 1 m below the lower flange of the specimen.

To evaluate the thermal behavior of the beam specimen and the reproducibility of the fire test in the NFRL, five individual tests were conducted on the same specimen under two different fire conditions provided by the natural gas burner. The first series of the tests was conducted by increasing the heat release rate in 100 kW increments approximately every 5 min (Tests 1 and 2); the second series of the tests utilized the heat release rate fixed at 400 kW throughout the test period (Tests 3, 4, and 5). All of the five tests were terminated when any one of the thermocouples installed at the specimen indicated about 500 °C.

Test data included the heat release rate of the burner, temperatures, adiabatic surface temperatures (to characterize thermal exposure), and displacements of the beam specimen. For temperature measurements, a total of fifty-three, type-K, 24 gauge thermocouples (tc) were installed at eleven different cross sections along the specimen length as shown in Figure 1. Four 25 mm linear position sensors were installed at 0.29 m from the beam ends to measure the axial displacements (thermal elongation). Two 50 mm linear position transducers were used to measure the vertical displacement induced by thermal bowing effects. For tests 3 through 5, four plate thermometers were installed to measure the adiabatic surface temperature at midspan of the beam specimen. A thermal imaging camera was used to record the spatial temperature distribution in the fire-exposed portion of the beam specimen.

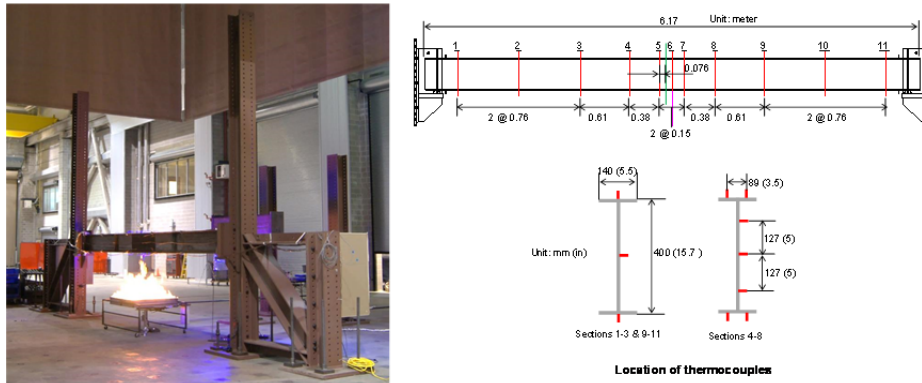


Figure 1. Fire-thermal test setup and thermocouple layout

Test results

Figure 2 shows the heat release rate output from the burner for each test and the corresponding temperature changes at the fire-exposed zone of the specimen. Temperatures shown herein are the average values to readings across sections 5, 6, and 7 at five different locations through the section depth. Six thermocouple readings were used to obtain the average temperature of the upper and lower flange and three thermocouple readings were used for each web temperature in Figure 2. No permanent deformation of the beam specimen was observed in the heating or cooling phase of the fire.

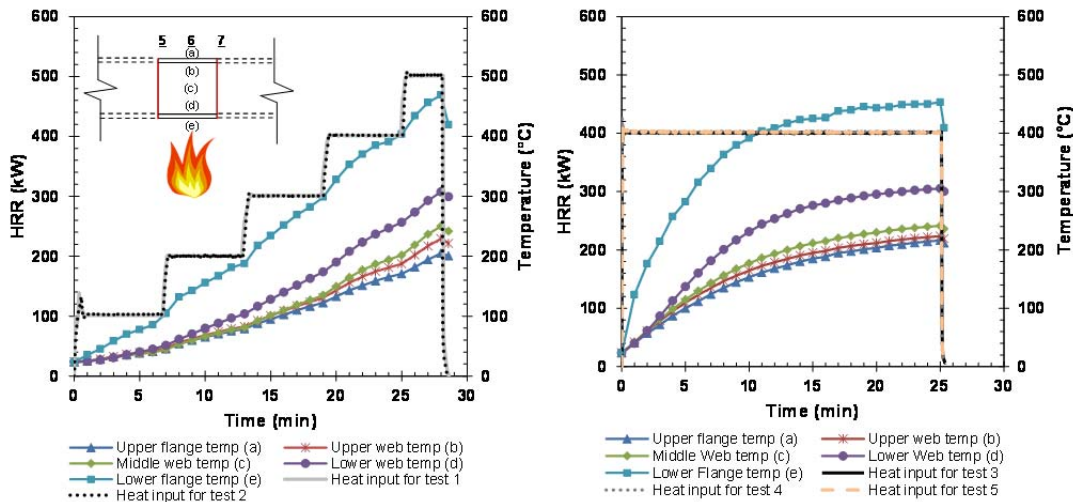


Figure 2. Heat input from the burner and steel temperatures at midspan[†]

When a step function was used to increase the heat source (i.e., HRR from the burner), it took approximately 28 min after ignition to reach the maximum discrete temperature of 500 °C at the lower flange of the specimen at midspan. The coefficient

[†] The estimated expanded uncertainty (U) of the temperature data is 20 °C (confidence interval of 95%) with U determined from a combined standard uncertainty ($u_c = 10$ °C) in the repeated temperature measurements at sections 5, 6, and 7 and the assumption that the possible estimated values of the standard are normally distributed with u_c .

of variation (COV) in the measured HRR from the two repeated tests (Tests 1 and 2) was 0.3%. The temperatures at the fire-exposed midspan of the beam specimen increased almost linearly until the fire was extinguished. A thermal gradient through the section depth was also exhibited. The temperature difference between the lower flange and the lower web (i.e., tc locations e and d, respectively, as shown in Figure 2) increased with increasing time of fire exposure, and reached 160 °C at 28 min. However, the maximum difference in temperatures at the upper portion of the cross section (along the tc locations a through c) remained below 25 °C.

When the burner was set to generate the constant HRR of 400 kW, it took approximately 25 min after ignition to reach the maximum discrete temperature of 500 °C at the lower flange of the specimen at midspan. The COV of the heat input from the three repeated tests (Tests 3, 4, and 5) was 0.2%. Unlike the previous tests, the temperatures at the exposed midspan of the specimen increased nonlinearly. The temperatures of the specimen increased rapidly following ignition, and then the rate of the temperature change decreased to slowly reach the steady-state regime. Thermal gradient through the section depth was also developed in a way that severe temperature gradients (as large as 150 °C) were observed in the lower portion of the exposed cross section, while small differences (≤ 17 °C) were exhibited in the temperatures of the upper portion.

Figure 3 shows the temperature distribution (at 11 different sections shown in Figure 1) along the specimen length before the fire was extinguished. Temperatures in this figure were the average values of tc readings from the repeated tests, with the expanded uncertainty ($\pm U$) indicated as error bars. U was estimated based on the estimated values of the standard[‡] (u_c) with a coverage factor of 2 (95% confidence interval). As shown in the figure, the thermal gradient along the beam length developed under two different fire conditions were similar. The constant HRR tests (Tests 3 through 5) showed a better representation of the symmetric thermal gradient with respect to the centerline of the beam specimen than the other tests (Tests 1 and 2).

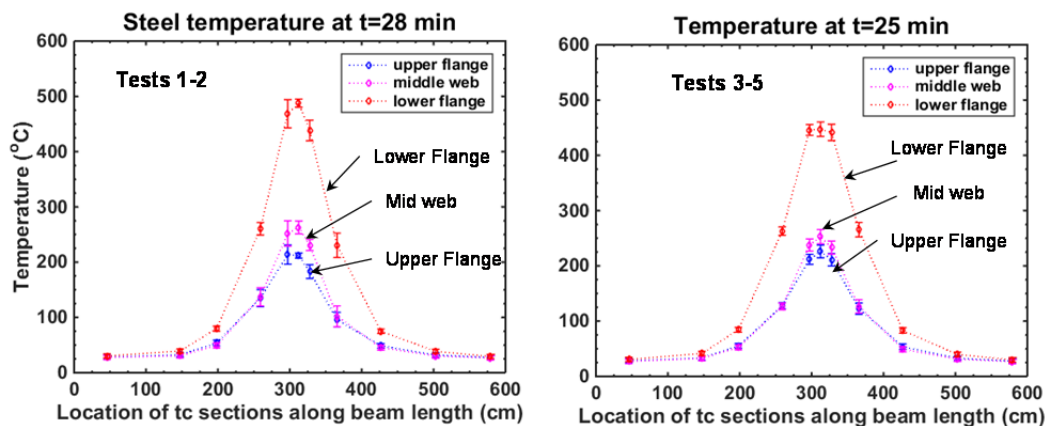


Figure 3. Thermal gradient along the beam length

[‡] The components of standard uncertainty (u_c) included test repeatability estimated using uniform distribution and manufactures' specifications on thermocouple error ($\pm 0.4\%$) and digitization error (± 3.2 °C) with 95 % confidence interval. Test repeatability was estimated using individual data points at specific tc locations (Figure 1) at a specific time of occurrence (t) after ignition. For sections 4 through 8 (Figure 1), there were two thermocouples at the upper and lower flanges each. These two tc readings were averaged to represent the upper and lower flange temperature at the specific location of the section.

STRUCTURAL FIRE TEST

Test setup, test protocol, and instrumentation layout

The W16×26 steel beam specimen was tested under combined flexural loading and a localized fire condition. Figure 4 shows the structural fire test setup. The same natural gas burner used in the fire-thermal tests was used to create a localized, open flame fire exposure directly to the critical sections (i.e., expected plastic hinge zone) of the specimen. For the structural loading, two hollow steel section (HSS) loading beams (placed on the top of the specimen) served as two point loads to produce a uniform bending moment across the fire-exposed critical sections of the beam specimen. The distance between the two loading points was 2.44 m (8 ft). The ends of the two HSS loading beams were connected to four 235 kN (53 kip) actuators via four 34.9 mm (1.38 inch) diameter high-strength steel rods. The high-strength steel rods had no rotational restraints at the ends. The actuators were mounted to the underside of the strong floor to protect them from fire. The HSS loading beams were water-cooled during the fire exposure.

The beam specimen was simply supported such that both end rotations about the principal axes and the axial (longitudinal) displacements were not restrained, whereas the beam ends were laterally restrained. The bearing-to-bearing length of the specimen was 5.87 m (19.25 ft). The room-temperature yield and ultimate strengths of the specimen were (440 ± 1.15) MPa and (530 ± 1.73) MPa, respectively[§].

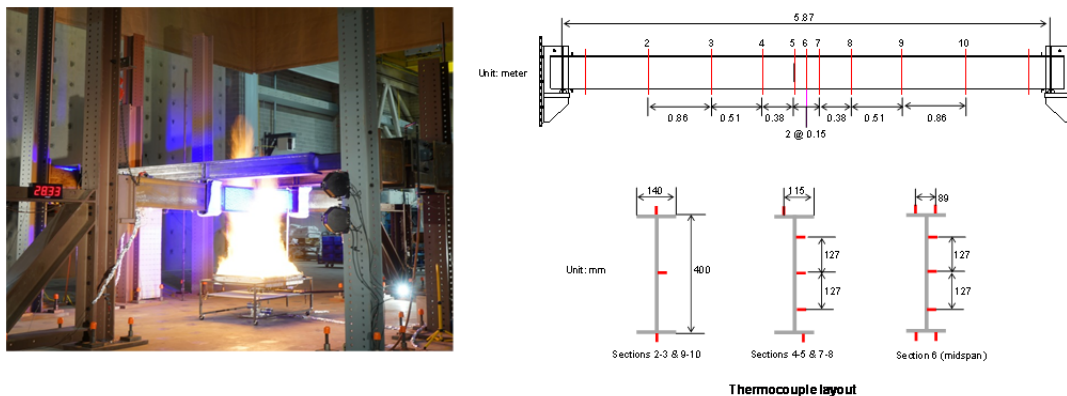


Figure 4. Structural fire test setup and thermocouple layout

The test was conducted in two steps as follows: (i) The HRR of the burner was increased to a target magnitude of 700 kW and maintained constant throughout the test. (ii) After the maximum temperature at the fire-exposed cross sections reached the steady-state condition, two point loads were programmed to increase at a rate of 2 kip/min (8.90 kN/min) simultaneously until the failure occurred.

For temperature measurements, a total of thirty nine, type-K, 24 gauge thermocouples were installed at nine different cross sections along the beam length as shown in Figure 4. Four plate thermometers and a thermal imaging camera were installed to supplement the temperature data of the specimen. The vertical and lateral

[§] The standard uncertainty (u_c) is estimated based on the certified material test report provided by steel fabricator and the assumption of uniform distribution. The numbers following the symbol \pm are the expanded uncertainty (U) with a level of confidence of approximately 95%.

displacements of the beam specimen in the fire-exposed zone were measured using specially designed potentiometers with temperature compensation. Two rotational transducers were installed at the specimen ends to measure the rotations about the principal axes of the beam cross section. The digital image correlation method was also used to measure the three-dimensional strains in the fire-exposed zone of the specimen. Technical details of the high-temperature displacement and strain measurements were not presented in this paper for brevity and because they are still under development. In addition to four actuators to apply and measure the structural loads, a 222 kN (50 kip) load cell were installed at each end of the beam specimen to measure the reaction forces during the test.

Test results

Figure 5 shows the test results including (i) the HRR data from the burner, (ii) the temperature data at the critical section (i.e., expected plastic hinge zone) of the specimen, (iii) the applied bending moment data, and (iv) the vertical displacement data at the fire-exposed midspan of the specimen. Note that the temperature data in Figure 5 are the average values of thermocouple readings of sections 5 and 6 only (Figure 4) and those of section 7 are not included as a result of flame lean during the test. The failed section was also located between the sections 5 and 6.

With the HRR-time relationship shown in Figure 5, the lower flange temperature reached steady-state at approximately 21 min. While the HRR of the burner was increased to 700 kW, no structural load was applied other than the self-weight of the specimen and the two water-filled HSS loading beam assemblies (16.7 ± 0.4 kN). The thermal gradient was developed through the cross sections, which resulted the thermal bowing about the strong axis.

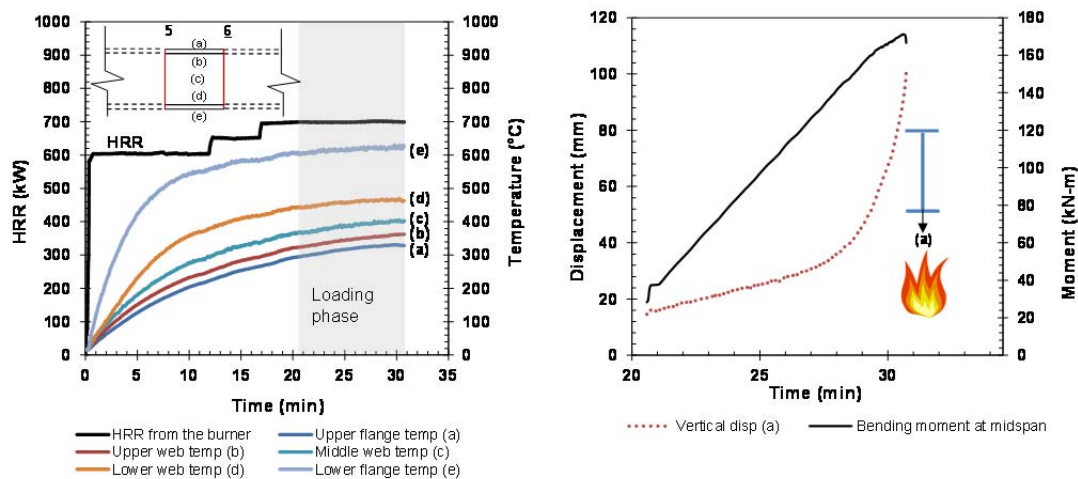


Figure 5. Fire-temperature and structural behavior of the beam specimen. **

** The temperature data has a maximum expanded uncertainty (U) of 34.0 °C calculated from a combined standard uncertainty (u_c) of 17.0 °C and a coverage factor of 2 (95 % confidence interval); The bending moment has U of 10.4 kN-m calculated from u_c of 5.2 kN-m and a coverage factor of 2. The vertical displacement data has U of 0.3 mm with a coverage factor of 2.

Under the loading phase where the HRR from the burner was maintained at a set point of 700 kW, the bending moment was applied at a rate of (14.7 ± 0.3) kN-m/min until failure occurred at approximately 31 min. The maximum temperature (at the lower flange at midspan) was (642 ± 28) °C, while the HRR was maintained at 700 kW. As shown in Figure 5, the vertical (downward) displacement of the beam specimen linearly increased with linearly increasing bending moments until the moment reached 124 kN-m (39 % of the plastic moment capacity at ambient temperature calculated using the plastic modulus in the steel manual [3]), then the nonlinear behavior was followed until failure. The increase in lateral displacements at midspan was also initiated at 124 kN-m. The measured peak moment capacity was 171 kN-m (54 % of the plastic moment capacity at ambient temperature) followed by runaway displacements. The failure was indicated by a sudden drop of the reaction force accompanied with rapidly increasing (runaway) displacements. As soon as the applied load and fire was removed, the beam specimen slightly bounced upward.

Figure 6 shows the photographs of the specimen at failure and the deformed shape of the specimen after cooling. Overall, when subjected to increasing flexural loads and the 700 kW fire, the beam specimen behaved in a complicated way that flexural bending and lateral torsional behavior were exhibited simultaneously.

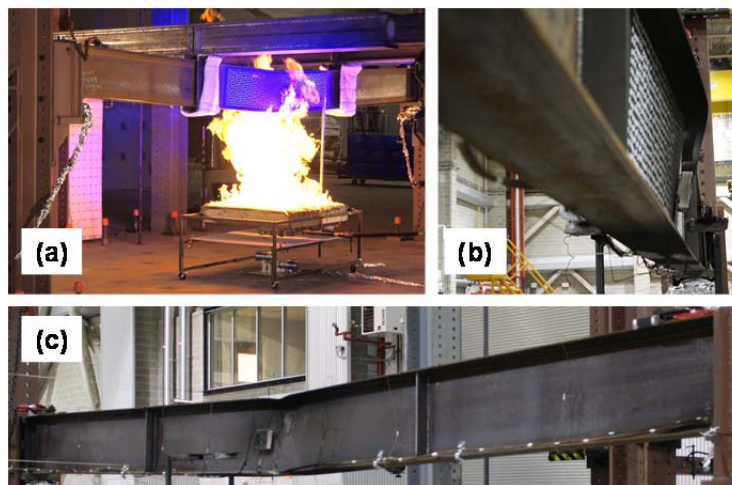


Figure 6. Photographs of (a) the beam specimen at failure, (b) the lateral-torsional deformation at the fire-exposed region, and (c) the beam specimen after cooling down.

SUMMARY

The open flame, localized fire tests were conducted on 6.17 m long W16×26 beams with simply supported boundary conditions. The experimental tests consisted of two parts: (1) fire-thermal tests to evaluate the effects of the prescribed heat release rates (HRR), provided by the 1 m × 1 m natural gas burner, on the thermal responses of the steel beam specimen and (2) structural-fire test to evaluate the effects of the localized fire on the behavior and the load-bearing capacity of the steel beam specimen. The cross sections at midspan (i.e., expected plastic hinge zone) of the beam specimen were directly exposed to a natural gas fire.

The test results indicated that the prescribed heat release rates from the burner affected the heating rate of the steel beam specimen. When the HRR-time relationship of the burner followed the step function with 100 kW increments approximately every 5 minutes, the temperatures at the fire-exposed region of the beam specimen increased linearly with increasing fire exposure time. When the HRR was set to a constant target magnitude of 400 kW, the specimen temperature indicated nonlinear heating to reach the steady-state condition. When the beam specimen was subjected to linearly increasing flexural loads at maintained HRR of 700 kW, combined flexural and lateral torsional failure of the specimen was exhibited. The peak moment capacity was achieved at 171 kN-m, which is 54 % of the plastic moment capacity at room temperature.

The test results from the present study can be used for developing or calibrating analytical models, which can be eventually used for evaluating the performance of structural members subjected to a localized fire. The findings from this study are limited to the range of parameters included in the tests. Further evaluation on the effects of various boundary conditions (axial and rotational restraints) and heating rates on the fire performance of the beam specimens are currently on going.

ACKNOWLEDGEMENT

The research presented in this paper was carried out under the NFRL Infrastructure and Commissioning project which seeks to deliver a fully operational NFRL, including outfitting of laboratory infrastructure and verifying operation and calibration of individual and combined fire and structural systems. We thank our colleagues Matthew Bundy, Anthony Chakalis, Artur Chernovsky, Learean DeLauter, Matthew Hoehler, Doris Rinehart, Brian Story, Christopher Smith, Nelson Bryner, and Jian Jiang who provided insight and expertise that greatly assisted the experimental research at NFRL or helped to improve the paper.

REFERENCES

1. Bundy, M., Hamins, A., Gross, J., Grosshandler W., Choe, L. 2016. "Structural Fire Experimental Capabilities at the NIST National Fire Research Laboratory," *Fire Technology*, pp. 1-8, doi:10.1007/s10694-015-0544-4.
2. ASTM International. 2015. "Standard Specification for Structural Shapes," Standard A992, ASTM International, W. Conshohocken, Pa.
3. AISC. 2010. Steel Construction Manual, 14th edition, American Institute of Steel Construction (AISC), Table 1-1, Chicago, IL
4. Bryant, R., Bundy, M., Zong, R. 2015. "Evaluating Measurements of Carbon Dioxide Emissions Using a Precision Source—A Natural Gas Burner," *J. the Air & Waste Management Association*, 65(7), pp, 863-870. doi: 10.1080/10962247.2015.1031294.